THE ASTROPHYSICAL JOURNAL, 448:788–796, 1995 August 1

NEBULAE AROUND LUMINOUS BLUE VARIABLES: A UNIFIED PICTURE

ANTONELLA NOTA, MARIO LIVIO, AND MARK CLAMPIN
Space Telescope Science Institute, 3700 San Martin Drive, Baltimore, MD 21218
AND
REGINA SCHULTE-LADBECK
Department of Physics and Astronomy, University of Pittsburgh, Pittsburgh, PA 15260
Received 1994 November 23; accepted 1995 February 3

ABSTRACT

The study of the nebulae around luminous blue variables (LBVs) provides clues to the mass-loss history of massive stars before and during the LBV phase. In this paper we investigate the possibility that the LBV nebulae (LBVNs) are shaped by interacting winds. We compare the morphologies of all known nebulae around LBVs, by compiling the results of our detailed coronagraphic imaging and spectroscopic studies of individual LBVs and their nebulae together with other relevant information from the literature. Most LBVs exhibit axisymmetric morphologies, suggesting that a single basic formation mechanism is involved. We propose that a model which consists of a stellar wind interacting with a preexisting density contrast (between the equatorial and polar directions) can explain most observed morphologies. There are several mechanisms which can produce the necessary density contrast, and at present it is difficult to determine definitively whether one or more of these mechanisms have been operating in the different systems.

Subject headings: stars: evolution — stars: mass loss — stars: variables: other (luminous blue)

1. INTRODUCTION

The luminous blue variables (LBVs) were first defined as a class by Conti (1984; see also Humphreys & Davidson 1994). The spectrophotometric variability of the LBVs exceeds (at times) that of other hot supergiants, and this is the main distinguishing characteristic of the class. Since the group is not defined by spectroscopic classification criteria, it might contain stars whose evolutionary states are unrelated. However, it is generally assumed that the LBVs represent a specific, important evolutionary phase in the lives of massive stars (cf. Langer et al. 1994). Several LBVs are located in the H-R diagram near the Humphreys-Davidson limit, suggesting that very massive stars do not evolve into red supergiants but reverse their redward evolution, after having lost a significant portion of their mass in the LBV stage, and become H-poor, Wolf-Rayet stars.

Six LBVs are currently known in the Galaxy: η Car, AG Car, HR Car, P Cyg, WRA 751, and HD 160529. The same number of LBVs has been recognized in the LMC: S Dor, R127, R71, HD 269582, R110, and R143. Another 20 LBVs are located in nearby galaxies (cf. Humphreys 1989). Since LBVs are rare, the LBV phenomenon must correspond to a short-lived evolutionary phase. The duration of the LBV phase has been estimated to be 1% of the main-sequence lifetime of a 40 $M_\odot$ precursor, or 4×10^4 yr (de Koter 1993), resulting in an expected number of about 60 LBVs in the Galaxy. The majority of LBVs are suspected to be as yet undiscovered because of limited photometric coverage of hot supergiants which might be quiescent LBVs.

The optical variability of LBVs is characterized by three different amplitude scales (Lamers 1987):

1. Microvariability of a few hundredths to a few tenths of a magnitude occurs on timescales of weeks to months, and is similar to that which is observed in other supergiants (van Genderen 1989). The spectra of LBVs display multiple, narrow absorption features on comparable timescales, which are indicative of sporadic mass ejections, probably in the form of blobs (e.g., Taylor et al. 1991). The microvariability might be related to the radiation-driven wind instability and triggered by pulsational instability common to all hot stars during shell-H burning (Langer et al. 1994). The mean mass-loss rate in the quiescent phase is estimated to be typically about 10^{-5} to 10^{-4} $M_\odot$ yr^{-1}. Terminal wind velocities depend on the spectral type, and are of order 200 km s^{-1} for B supergiants and greater than 200 km s^{-1} for O and Ofpe/WN9 transition-type stars.

2. Moderate, cyclic variability with amplitudes of 1–2 mag and with timescales of years to a decade is a unique type of variability observed in LBVs. A historically quiescent hot supergiant becomes an LBV once this type of variation has been recorded. The photometric and spectroscopic behavior of LBVs during a moderate-variability cycle can be explained with radius and temperature changes at constant bolometric luminosity. During optical minimum, when the stars are hottest, they have the smallest radii, and during optical maximum, when they are coolest, they have the largest radii. The terminal wind velocities drop to around 100 km s^{-1} when LBVs are in their cool, A-type state.

Drastic variations in the physical structure of the stars and/or in the stellar atmospheres must be taking place during a moderate-variability cycle, and two different scenarios have been proposed. The onset of an excursion toward lower temperatures could be due to a significant (but unexplained) increase in the stellar mass-loss rate, which, because of increased optical depth in the wind, leads to the formation of an extended "pseudo-photosphere" (e.g., Davidson 1987; Lamers 1987). Or the variations could mainly be due to true (but also unexplained) radius variations of the star (Leitherer et al. 1989). Thus, the question of whether or not the mass-loss rate changes with respect to the quiescent state is crucial for distinguishing between these two models.

3. Giant eruptions with changes in visual brightness by more than 3 mag, and lasting for decades, have been observed

in two Galactic LBVs, η Car (1837–1860) and P Cyg (1600–1660), and in the extragalactic LBV V12 in NGC 2403. Giant eruptions are believed to be associated with significant mass ejections, of order 10^{-2} to 1 $M_\odot$. The "homunculus" nebula around η Car is the prominent, visible remnant of η Car's giant eruption, and it contains about 2 $M_\odot$ (Davidson 1989). The mass-loss rate was very large during the eruption, of the order 10^{-1} $M_\odot$ yr^{-1}. The nebulosity around P Cyg is much less spectacular than that around η Car, and it was only recently resolved by imaging (Barlow et al. 1994; Clampin et al. 1995a). The total mass ejected by P Cyg in its giant eruption was about 10^{-2} $M_\odot$, hence its mass-loss rate was probably between 10^{-4} and 10^{-3} $M_\odot$ yr^{-1}. P Cyg has been extremely quiet since its giant eruption and would not have been classified as an LBV if it were not for that event.

Since giant eruptions have not been observed in all LBVs, it is possible that either the timescales between giant eruptions are so long, of the order of centuries, that they have not yet been observed in all LBVs, or that not all LBVs experience giant eruptions. Other LBVs are, however, inferred to have had giant eruptions from the presence of extended nebulosity around them. Examples for such objects are AG Car, HR Car, and R127. As in the case of η Car, the nebulae around these LBVs contain up to a few solar masses (see below). Nebular expansion velocities have been used to derive nebular ages, which turn out to be of the order of several thousand years, hence these nebulae are older than the homunculus. It should be noted that these ages are also a significant fraction of the anticipated duration of the LBV phase. More recently, the presence of a ring nebula has been used to advance some hot supergiants to LBV candidacy, even in cases in which their photometric variability history is completely unknown. Thus, Smith, Crowther, & Prinja (1994) proposed He 3-519 as a Galactic candidate, and Nota et al. (1994) identified the LMC candidate S119.

The mechanism responsible for the giant eruptions has been potentially linked to a pulsation instability. Most recently, Langer et al. (1994) identified a phase of violent radial pulsational instability in stellar models, when a very massive (>40 $M_\odot$) star during shell-H burning evolved toward surface temperatures below 20,000 K. In the instability regime, the mass-loss rate of their 60 $M_\odot$ model star was 5×10^{-3} $M_\odot$ yr^{-1}, and the star lost a total of 6 $M_\odot$, until it again evolved to hotter temperatures.

The morphology of the nebulae around LBVs provides clues to the mass-loss history of massive stars before and in the LBV phase. In this paper we shall investigate the hypothesis that the LBV nebulae (LBVNs) are shaped by some form of interacting winds. Guided by work done on the morphology and formation mechanism of planetary nebulae (PNe) (Balick 1987), we shall attempt to point out similarities in the morphologies of LBVNs to PNe, which will provide insight into the formation mechanism of LBVNs. Morphological similarities between PNe and LBVNs have been noted before (e.g., by Chu 1993). We shall put this comparison on a firm observational footing, by compiling the results of our detailed coronagraphic imaging, spectroscopic, and spectropolarimetric studies of individual LBVs and their nebulae (see references given in Table 1), together with other relevant information from the literature. These data will allow both an intercomparison of the physical properties of LBVNs and a comparison with PNe. The data are described in § 2, our unified model is presented in § 3, and conclusions follow.

2. A COMPARISON OF THE OBSERVED PROPERTIES

Many LBVs display circumstellar nebulae. The nebulae around η Car and AG Car are relatively bright and extended and, consequently, have been known since the 1950s (Thackeray 1950). Other smaller and fainter nebulae have only been discovered more recently from the presence of nebular lines in their spectra, and subsequently have been imaged. Coronagraphy has facilitated a significant step forward in the detection and morphological study of these nebulae, which are very difficult to study with conventional imaging techniques (Clampin et al. 1993). The first results obtained with stellar coronagraphs prompted multiwavelength follow-up studies (such as spectropolarimetry), and much progress has been made in this field over the past 10 years. In the next subsections we will review the current status of observations of nebulae around LBVs by comparing their reported properties and exploring their similarities and differences. An overview of the observations of nebulae around known and suspected Galactic and LMC LBVs is summarized in Table 1, drawing on our own observations and the literature for its sources. The individual observational parameters are now discussed in turn.

2.1. *Morphology*

The study of the nebular morphology has allowed us to group LBVs into three main categories:

1. *Shell nebulae.*—The majority of LBVs are surrounded by shells, usually with enhanced brightness regions aligned to a preferred axis of symmetry. LBV shell nebulae are found to exhibit split nebular lines, indicating that the shells are mostly hollow, and they are expanding. Typical objects which can be assigned to this category are the Galactic LBV AG Car, and R127 in the LMC; the Galactic LBV candidates HD 168625, He 3-519, and S119 in the LMC. We include in this category also the nebula around the Galactic LBV WRA 751, although no detailed information on its nebular morphology is yet available, and η Car, which exhibits, in PN terminology, a *true* bipolar nebula with the homunculus at its core.

2. *Filamentary nebulae.*—We include in this class the nebulae surrounding the Galactic LBV HR Car and the newly discovered R143 in the LMC.

3. "*Peculiar*" *morphologies.*—In this category we include P Cyg, where the nebula is composed of a distribution of "blobs" within a spherically symmetrical nebula.

Let us examine these categories one at a time, in the attempt to outline similarities and differences, and possibly to identify common elements in the nebula formation mechanism and evolution.

2.1.1. *Shell Nebulae*

AG Car is surrounded by an elliptical nebulosity which is $39'' \times 30''$ in size, which, given the recently revised distance of 6 kpc (Humphreys et al. 1989), translates into a linear dimension of 1.1×1.0 pc. The optical morphology suggests a bipolar structure. Such a structure is evident from the V-band images, which show starlight reflected by dust negligibly contaminated by the nebular continuum, and from the nebular line ([N II], Hα) images (Stahl 1987; Nota et al. 1992), which show the distribution of ionized gas (Figs. 1 and 2 [Pl. 28]). In the emission-line images, the nebula appears to be composed of two elongated, nested ring structures. The gas density is strongly enhanced in the southwest and northeast directions.

1995ApJ...448..788N

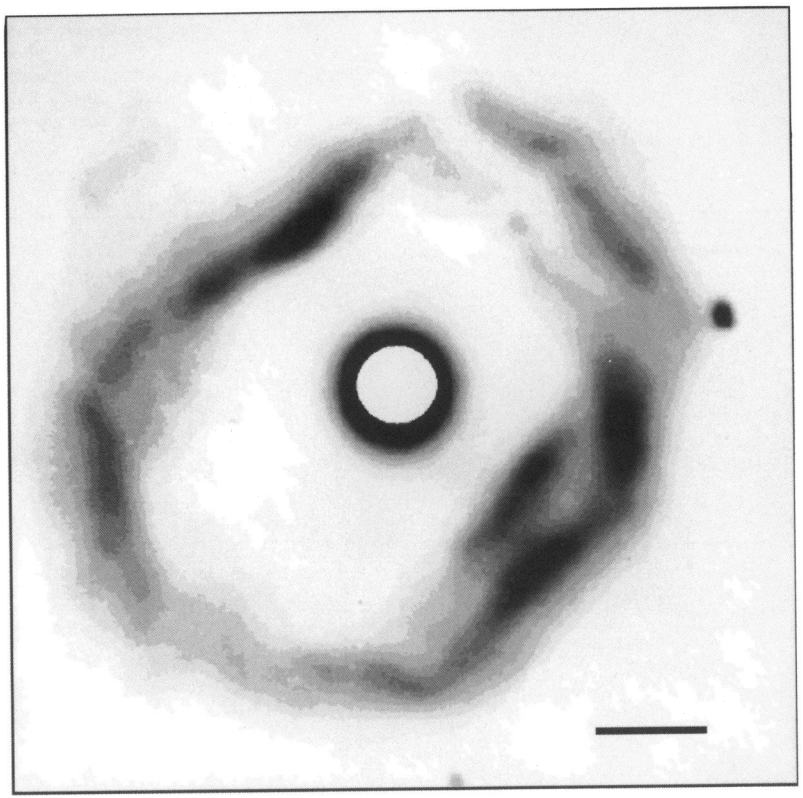

FIG. 1

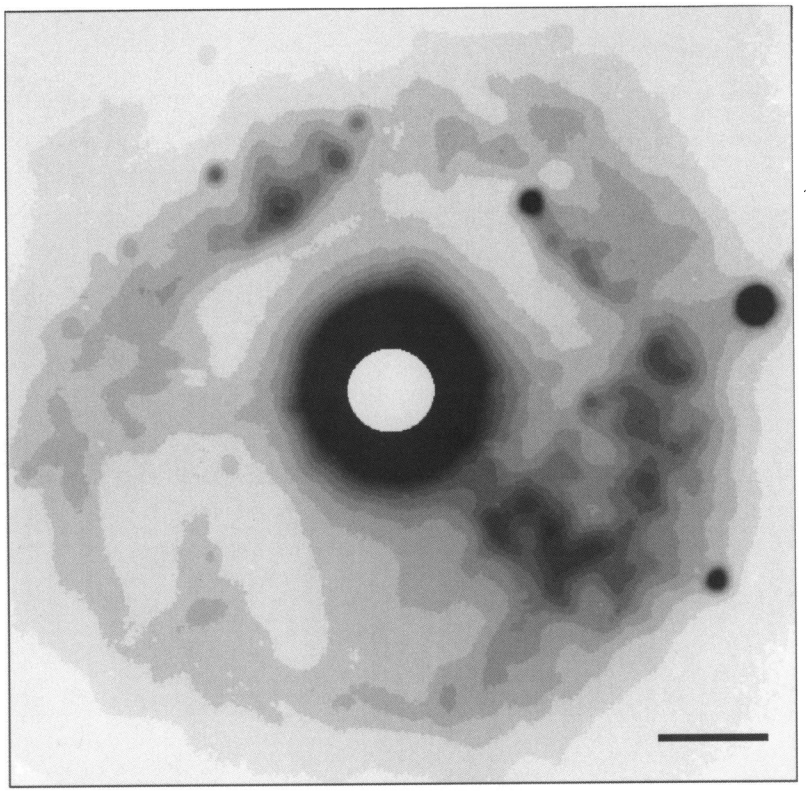

FIG. 2

FIG. 1.—*R*-band image of AG Car obtained with the STScI Coronagraph, where north is at the top and east is to the left. The scale bar at the bottom right is 5″ long, and the star is occulted by a 3″ diameter mask, which has been artificially enlarged to 3″.8.

FIG. 2.—Hα + [N II] narrowband image of AG Car obtained with the STScI Coronagraph, where north is at the top and east is to the left. The scale bar at the bottom right is 5″ long, and the star is occulted by a 3″ diameter mask, which has been artificially enlarged to 3″.8.

NOTA et al. (see 448, 789)

TABLE 1

PROPERTIES OF NEBULAE AROUND LBVs AND RELATED OBJECTS

Star (1)	Spectral Type (2)	M_{bol} (3)	V (km s^{-1}) (4)	Nebular Size (pc) (5)	v_r (km s^{-1}) (6)	Dynamic Time (yr) (7)	M_{gas} ($M_\odot$) (8)	M_{dust} ($M_\odot$) (9)	N_e (cm^{-3}) (10)	T_e (K) (11)
AG Car.....	A1 I[a]–Ofpe/WN9[b]	−10.8[c]	80–250[d]	1.1 × 1.0[e]	70[f]	8.4 × 10^3 [f]	4.2[e]	0.013[g,h]	800[i]	9000[i]
R127	B5–Ofpe/WN9[j]	−10.3[k]	~150[l]	1.9 × 2.2[m]	28[n]	4 × 10^4 [m]	3.1[m]	...	1000[o]	...
η Car	20,000–30,000 K[p]	−12.5[p]	...	0.2[q]	600[r]	150[s]	...	0.01[t]	...	[t]
He 3-519	WN11[g]	−7.1[g]	365[g]	2.28[g]	61[g]	1.8 × 10^4 [g]	2.0[g]	0.0066[g]	300[g]	8000[g]
S119	Ofpe/WN9[u]	...	...	1.9 × 2.1[v]	25[v]	5 × 10^4 [g]	1.7	...	800[v]	...
WRA 751	O9.5[w]	−9.6[w]	...	0.8[h]	20–60[x]	...	...	...	...	...
HD 168625.....	B2–B8[y]	−8.6[y]	250[y]	0.06[y]	20[y]	3 × 10^3 [y]	0.03[y]	0.0003[h,y]	630[h,y]	...
HR Car.....	B2 I–B9 II[z]	−9.4[z]	145–170[z]	0.98[aa]	50[z]	10^4 [z]	2.1[aa]	0.0010[h]	600[z]	<12500[z]
R143	B1 I–F8 I[bb]	−10.2[bb]	...	3.5[bb]	...	...	...	...	...	...
P Cyg.....	B1 Ia+[cc]	−8.3[dd]	206[dd]	0.2[dd]	140[dd]	10^2–10^3 [dd]	0.0092[dd]	...	1000[dd]	5000[dd]

NOTE.—The nebulae are listed in the order in which they are presented in the text. For each object, we indicate the name of the central star (col. [1]); its most extreme spectral types recorded (col. [2]); its bolometric magnitude M_{bol} (col. [3]); its wind velocity V (col. [4]); the size of the surrounding nebula (col. [5]); the nebular expansion velocity v_r (col. [6]); the dynamic time associated with the expansion velocity (col. [7]); the mass of ionized gas contained in the nebula (col. [8]); the mass of dust contained in the nebula (col. [9]); the electron density (col. [10]); and the nebular temperature (col. [11]). All the parameters given are referenced, and the references are listed in footnotes below.

[a] Caputo & Viotti 1970.
[b] Stahl 1986.
[c] Humphreys et al. 1989.
[d] Leitherer et al. 1994.
[e] Nota et al. 1992.
[f] Smith 1991.
[g] Smith et al. 1994.
[h] Hutsemekers 1994.
[i] Mila Mitra & Dufour 1990.
[j] Walborn 1977.
[k] Wolf 1989.
[l] Wolf et al. 1988.
[m] Clampin et al. 1993.
[n] Appenzeller et al. 1987.
[o] Stahl & Wolf 1986.
[p] Davidson et al. 1986.
[q] Humphreys & Davidson 1994.
[r] Allen & Hillier 1993.
[s] Walborn et al. 1978.
[t] Davidson 1989.
[u] Bohannan & Walborn 1989.
[v] Nota et al. 1994.
[w] Hu et al. 1990.
[x] de Winter et al. 1992.
[y] Hutsemekers et al. 1994.
[z] Hutsemekers & Van Drom 1991a.
[aa] Clampin et al. 1995c.
[bb] Parker et al. 1993.
[cc] De Groot 1969.
[dd] Barlow et al. 1994.

The two locations of enhanced gas density are found to be in correspondence with the highest dust density regions. Newly obtained images of the AG Car nebula, taken with the WFPC2 on *HST* in a narrow V continuum, show the overall bipolar dust distribution and resolve the structure which was commonly referred to as the "jet" into filaments, arcs, loops, and bubbles organized in a complex structure (Nota et al. 1995).

R127 in the LMC is very similar to AG Car. The linear size of the nebula is slightly larger, 1.9 × 2.2 pc, assuming a distance to the LMC of 51.2 kpc (Panagia et al. 1992), but the overall morphology is the same (bipolar). The R127 nebula, originally detected by Stahl (1987), has been resolved in coronagraphic images taken in the light of Hα + [N II] by Clampin et al. (1993) and appears diamond-shaped, with two compact, bright lobes located east and west with respect to the star, and two much fainter ansae in the north and south regions (Fig. 3 [Pl. 29]). Fainter, extended emission is detected in the east region, extending up to 30″ from the star.

The η Car nebula is the best example of a bipolar, axially symmetric outflow (Fig. 4 [Pl. 29]). Two hollow (Allen & Hillier 1993), bipolar lobes appear well defined in a recent set of *HST* pictures taken in continuum light (Humphreys & Davidson 1994; but see also Ebbets et al. 1992, 1993). Other material appears concentrated in an "equatorial waist," including several radially elongated streaks and large clumps. One "jetlike" feature is visible to the northeast of the core, and another similar feature is superposed on the northwest lobe. Equatorial radial streaks are observed, which move outward with measured velocities up to 1500 km s^{-1}. They might be the fragments of a protostellar disk, or may represent ablation from a much smaller and denser equatorially compressed circumstellar disk (see § 3.2).

He 3-519 has been recently studied by Davidson et al. (1993) and Smith et al. (1994). The nebula is much larger than the other LBV nebulae mentioned so far: 2.28 pc in diameter (under the assumption of a distance of 8 kpc). As in the case of AG Car (Humphreys et al. 1989), the distance of He 3-519 has recently been revised from the 2.5 kpc originally determined by Stahl (1986), on the basis of kinematic and reddening versus distance considerations. From the narrowband images, He 3-519 appears as a simple, symmetrical, hollow shell (Stahl 1987; Smith et al. 1994). However, its velocity structure is more complicated, and the spherical expansion appears to be distorted in the southern region. No observations exist yet of the inner nebula, which could potentially provide evidence of an asymmetric flow.

The nebula around S119 in the LMC also looks like a shell. S119 is a Ofpe/WN9 star for which little information is available in the literature, apart from the discovery paper (Bohannan & Walborn 1989). The presence of the nebula was first inferred from the observations of typical nebular lines [N II] in high-resolution optical spectra (Nota et al. 1994). Subsequent coronagraphic imaging showed a nebula of size and mass just smaller than R127 ($\simeq 1.7\ M_\odot$; see Table 1), with a morphology very similar to that of AG Car and R127, 7″ × 9″ in size, corresponding to 1.9 × 2.1 pc^2 (Fig. 5 [Pl. 30]). An asymmetry in the shell brightness is visible along the northeast-southwest axis, with a very bright lobe extending toward the northeast up to 4″ from the star.

WRA 751 is a newly discovered LBV (de Winter et al. 1992): evidence of a nebula is noticed in direct images taken in the light of Hα and in the infrared Gunn z. The geometry of the nebula appears quite circular in all the images, but its detailed shape is unresolved. Assuming a distance of 7.1 kpc

1995ApJ...448..788N

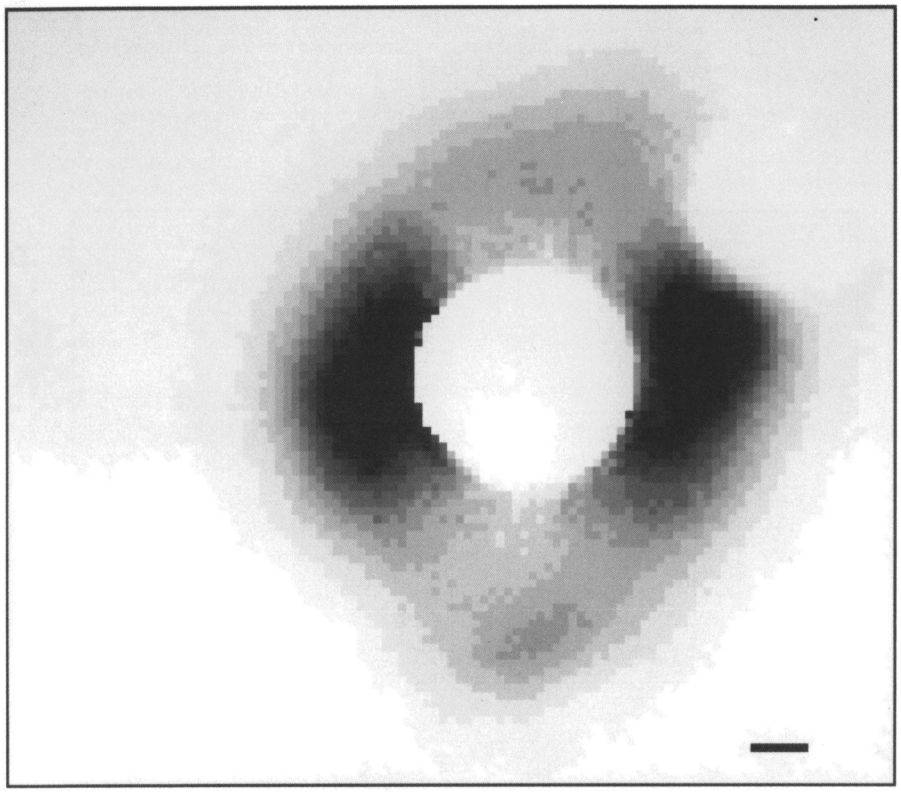

FIG. 3

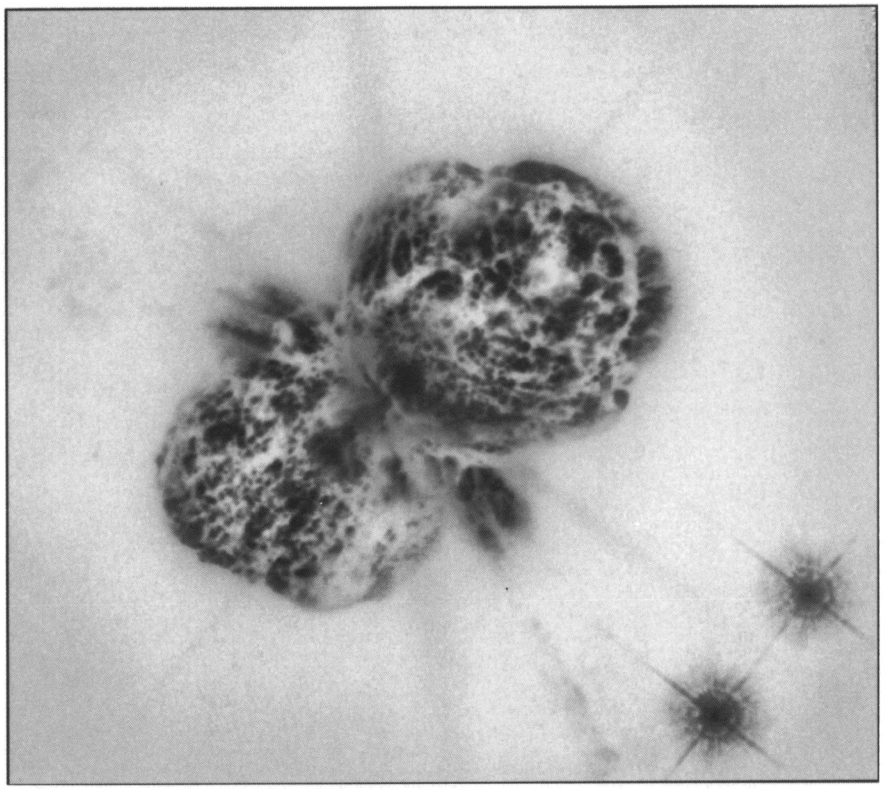

FIG. 4

FIG. 3.—An 1800 Hα + [N II] image of R127, obtained with the Johns Hopkins Adaptive Optics Coronagraph. The scattered light contribution due to R127, its companion R127B, and the field stars have been subtracted. The scale bar is 1″ long; north is at the top east is to the left.

FIG. 4.—*HST*/WFPC2 image of η Car, taken with a *U* filter. The image is the composition of several short (2 s) and long (40 s) exposures. The width of the image is 22″. The contrast has been enhanced via an adaptive algorithm. (Courtesy of Dennis Ebbets and Rick White.)

1995ApJ...448..788N

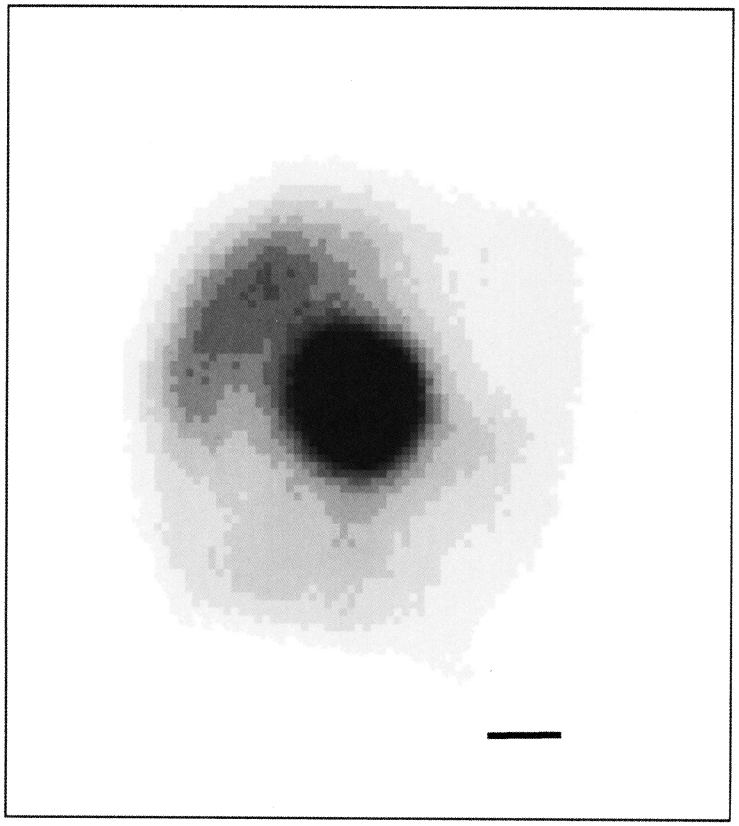

FIG. 5

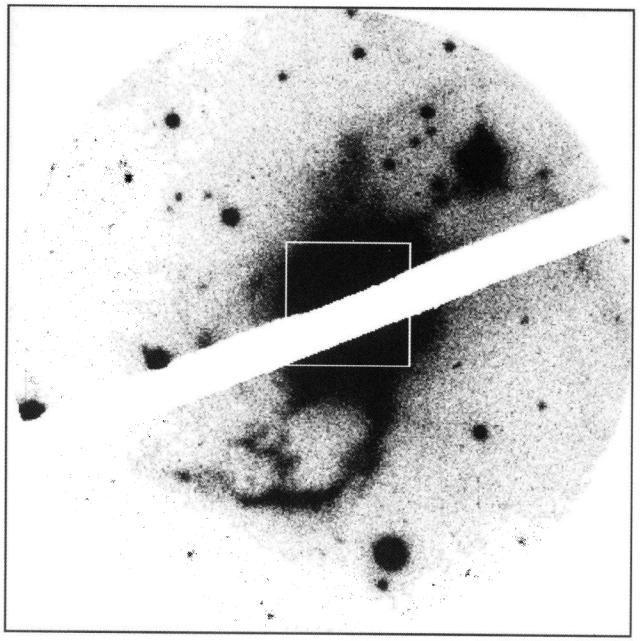

FIG. 6

FIG. 5.—[N II] image of the S119 nebula taken with the STScI Coronagraph. The central star is not occulted in this image, although the contrast in the circumstellar region is still enhanced by pupil apodization. North is at the top and east is to the left, and the scale bar in the image is 1″ long.

FIG. 6.—An 1800 [N II] image of HR Car, taken with the STScI Coronograph. North is at the top and east is to the left. The field of view in the main image is 50″ in diameter, and the inset image shows the central 10″, at a different contrast to illustrate the features in the inner nebula.

NOTA et al. (see 448, 790 and 791)

(Hutsemekers 1994), the linear radius of the nebula is 0.40 pc, again very similar to AG Car. Unfortunately, is is not possible to comment on the detailed morphology.

HD 168625 is a candidate LBV (Hutsemekers et al. 1994). It is a very luminous B-type supergiant, whose spectral variations between B2, B8, and B5.6 have been recorded on a baseline of more than 40 years. Its spectrum shows the characteristic P Cygni profiles in Hα, with a wind terminal velocity of $\simeq 250$ km s^{-1}, very typical of LBVs. It is surrounded by a nebula which seems to consist of two shells: a first inner shell, 10″ × 13.″5 in diameter, appears to be oriented (in the Hα + [N II] images taken by Hutsemekers et al. 1994) with the major axis along the northwest-southeast direction. A second, larger ring, partially overlapping, is oriented along a perpendicular direction.

2.1.2. *Filamentary Nebulae*

HR Car's nebula is filamentary: discovered by Hutsemekers & van Drom (1991a) and subsequently imaged with a coronagraph by Clampin et al. (1995b), HR Car displays a bipolar, nearly point-symmetric structure, similar to some well-known planetary nebulae (e.g., NGC 6309; Schwarz, Corradi, & Melnick 1992). The two arcs discovered originally by Hutsemekers & Van Drom (1991a) have been found to be filaments which extend up to 18″ from the star ($\simeq 0.49$ pc, if a distance of 5.1 kpc is assumed). These filaments can be followed, in the coronagraphic images, down to 2″ from the star, where they merge in a bright, clumpy inner nebula. Fainter arcs have been identified by Clampin et al. (1995b), all of which originate within the same clumpy structure but then change position angle with distance from the star into a circular path, so that the overall impression is that of a spiral pattern (Fig. 6 [Pl. 30]).

R143 is a newly discovered LBV, the first in the central cluster of S Dor (Parker et al. 1993). The star has been observed to vary from a type F5–F8 supergiant to possibly O9, and now back to a late B supergiant, over a timescale of $\simeq 40$ years. It is surrounded by a circumstellar nebula; although no detailed chemical abundance or dynamical analysis has been done on the nebula, we will assume the nebula is physically connected to the star. The nebula appears filamentary in a very similar fashion to HR Car: the most striking difference is possibly that, in the case of R143, the four major filaments all seem to emerge from the star in the northern region. They also seem to curve with distance from the star, in a way that is reminiscent of the spiral pattern observed around HR Car, but each filament ends in a bright unresolved knot of emission. New coronagraphic imaging by Clampin et al. (unpublished) shows that, in addition to the above-mentioned filaments, more [N II] emission is visible in the close surroundings, in the form of blobs and diffuse regions (Fig. 7 [Pl. 31]). Contamination from an underlying H II region is possible.

2.1.3. "*Peculiar Nebulae*"

Only one object presently belongs to this category, which for the peculiarity of its appearance cannot be included in any of the above-mentioned groups: P Cyg.

Barlow et al. (1994) and Clampin et al. (1995a) both find that the nebula around P Cyg, in addition to being faint and, consequently, difficult to observe, is mainly composed of unresolved clumps of emission, distributed within a circular envelope. The diameter of the envelope is approximately 22″, which, at a distance of 1.8 kpc, corresponds to 0.2 pc. Two fainter, outer arcs are found by Barlow et al. (1994) with angular diameters of 1′ and 1.′5 from the star. Asymmetry is noticeable in the distribution of the brighter clumps, which seem to be more concentrated in the northern nebular hemisphere, although fainter clumps are observed everywhere within the circular envelope. The clumps are typically 2″–3″ in diameter, which would translate into a linear scale of $\simeq 0.022$ pc (Fig. 8 [Pl. 31]). The clumps appear very similar in shape and size to some features observed in the ground-based coronagraphic pictures of AG Car's dusty nebula, which have been recently resolved by *HST* imaging (Nota et al. 1995) into unexpected "cometary tails" and hollow bubbles (Fig. 9 [Pl. 32]).

As we can see from these detailed descriptions, most LBVNs show axial symmetries: from the clear-cut case of the bipolar outflow around η Car to the opposite extreme, P Cyg, in which an overall circularly symmetric nebula contains an asymmetric distribution of clumps. A variety of intermediate cases is observed. However, all LBVNs display some degree of axial symmetry, more evident in the shell nebulae (AG Car, R127, S119) but still visible in the other described objects (HR Car, R143).

2.2. *Expansion Velocity, Dynamical Timescale*

The dynamical timescale does not vary significantly across our sample: most nebulosities around LBVs were ejected typically 10^4 years ago. This number is derived by measuring the expansion velocity of the nebulae. It varies in the range 3×10^3 yr for HD 168625 to 5×10^4 yr for S119. It is interesting to note the much shorter dynamical timescale associated with the two "*youngest*" LBVNs, η Car and P Cyg. For η Car, Walborn, Blanco, & Thackeray (1978) measured proper motions for discrete features in the outer shell on plates taken at two different epochs, and from the deduced tangential velocities they derived a dynamical timescale of 10^2–10^3 yr. A subsequent study by Walborn & Blanco (1988), using third-epoch proper-motion measurements, suggested that the slowest material around η Car underwent significant deceleration. Therefore, most or even all of the material may have been ejected about 150 years ago during the high visual maximum of the 1830s and 1840s. In the case of P Cyg, Barlow et al. (1994) find that the [N II] emission knots observed in its circumstellar region are moving out at a velocity of 110–140 km s^{-1}, while P Cyg's wind currently has a velocity of $\simeq 200$ km s^{-1} (Exter 1994). Assuming that the observed expansion velocity remained constant over time, the dynamical timescale associated with the knots would be of the order of 800 yr, implying a major outburst a few hundred years before P Cyg's discovery (ca. A.D. 1600; De Groot 1969). This possibility cannot be ruled out, but it leaves open the question of the detection of the remnant of the series of outbursts recorded in the seventeenth century.

2.3. *Nebular Masses*

For all the nebulae for which we have coronagraphic imaging, we have determined the mass of ionized gas from the integrated Hα flux, after extinction correction (assuming a temperature and density either derived by us independently or taken from the literature). In Table 1 we list the nebular masses for our sample, and we also list the values of the temperature and density used in the calculations, quoting their source. For the nebulae for which we do not have narrowband images, we list the values in the literature. It is interesting to note that we find all the shell nebulae to have comparable masses within the uncertainties, which can be in some cases as high as a factor of

1995ApJ...448..788N

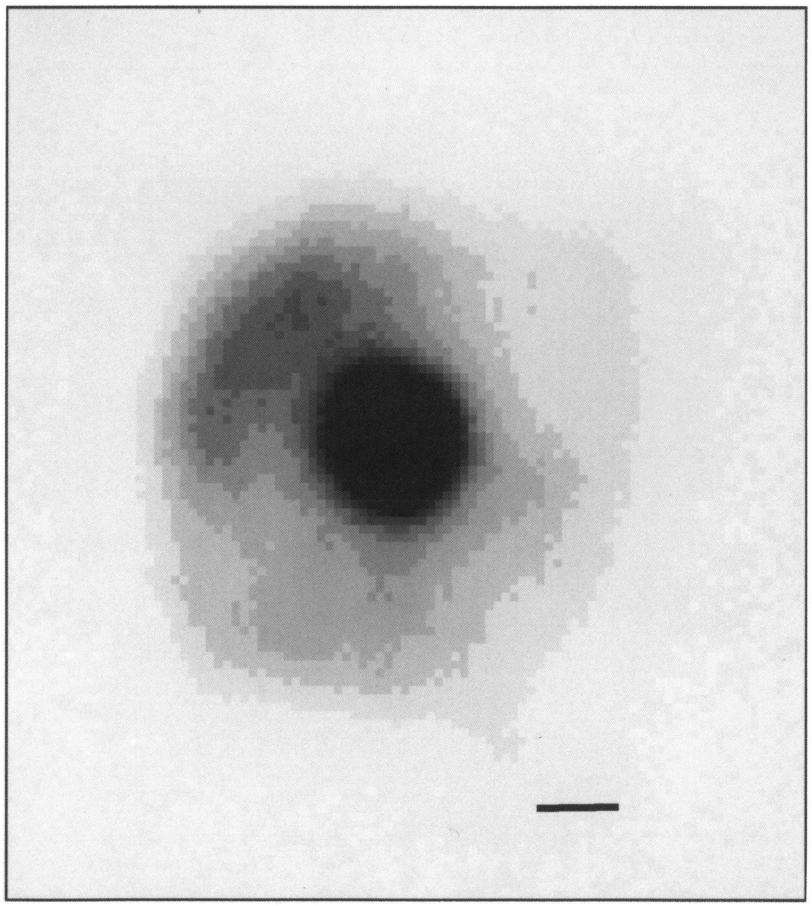

FIG. 5

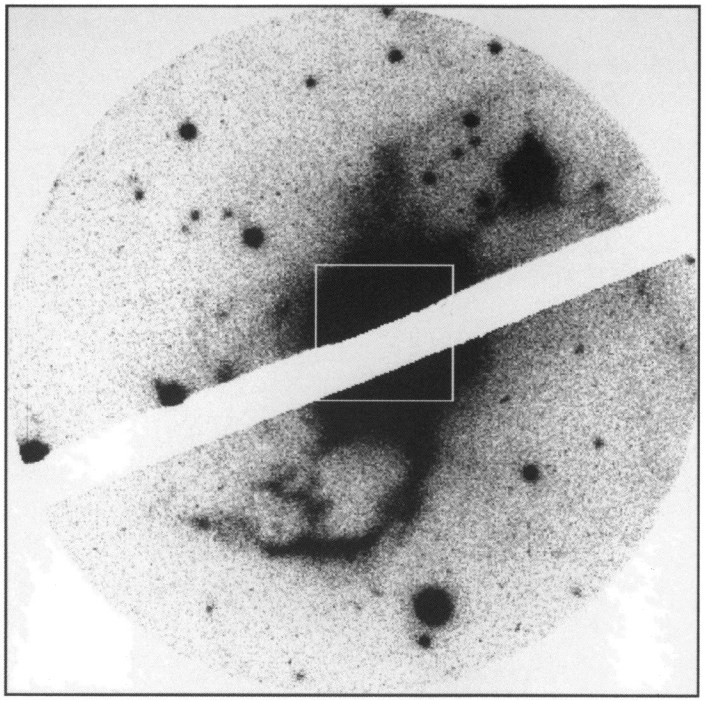

FIG. 6

FIG. 5.—[N II] image of the S119 nebula taken with the STScI Coronagraph. The central star is not occulted in this image, although the contrast in the circumstellar region is still enhanced by pupil apodization. North is at the top and east is to the left, and the scale bar in the image is 1″ long.

FIG. 6.—An 1800 [N II] image of HR Car, taken with the STScI Coronograph. North is at the top and east is to the left. The field of view in the main image is 50″ in diameter, and the inset image shows the central 10″, at a different contrast to illustrate the features in the inner nebula.

NOTA et al. (see 448, 790 and 791)

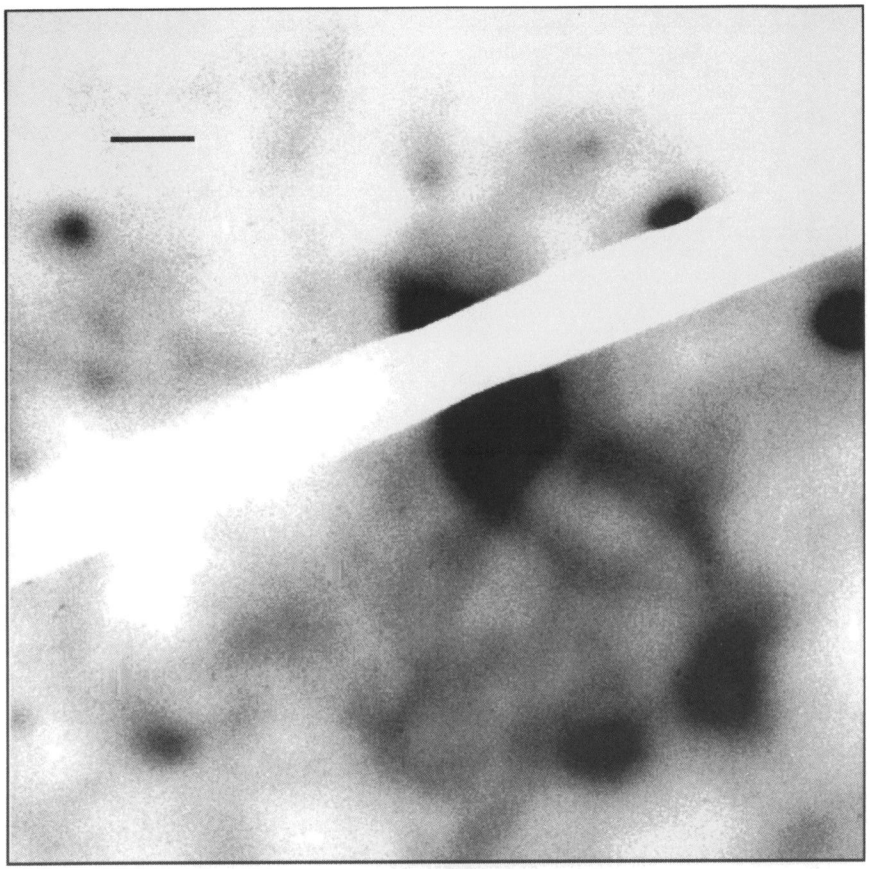

FIG. 7

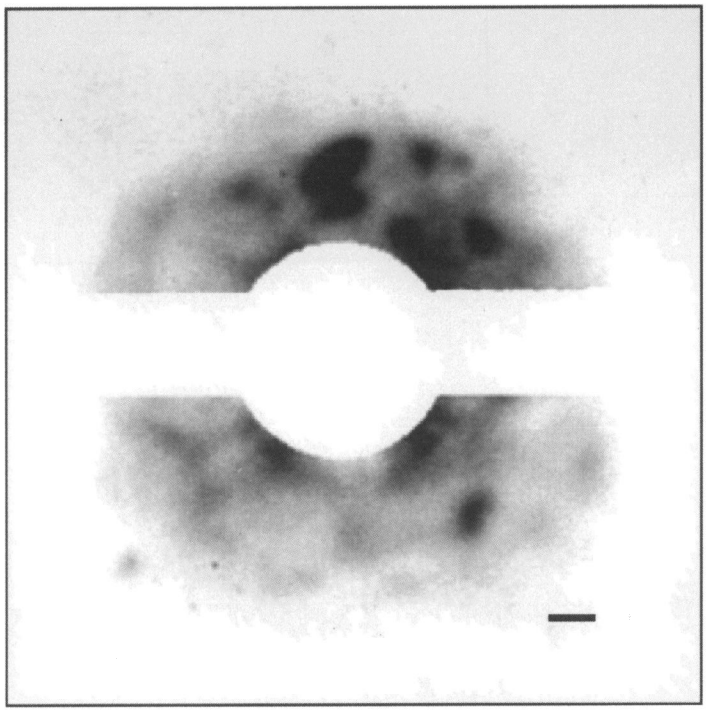

FIG. 8

FIG. 7.—An 1800 Hα image of R143a taken with the STScI Coronagraph. North is at the top east is to the right, and the scale bar in the image is 3″ long.
FIG. 8.—An 1800 [N II] image of P Cyg, taken with the STScI Coronagraph. North is at the top and east is to the left, and the scale bar is 2″ long.

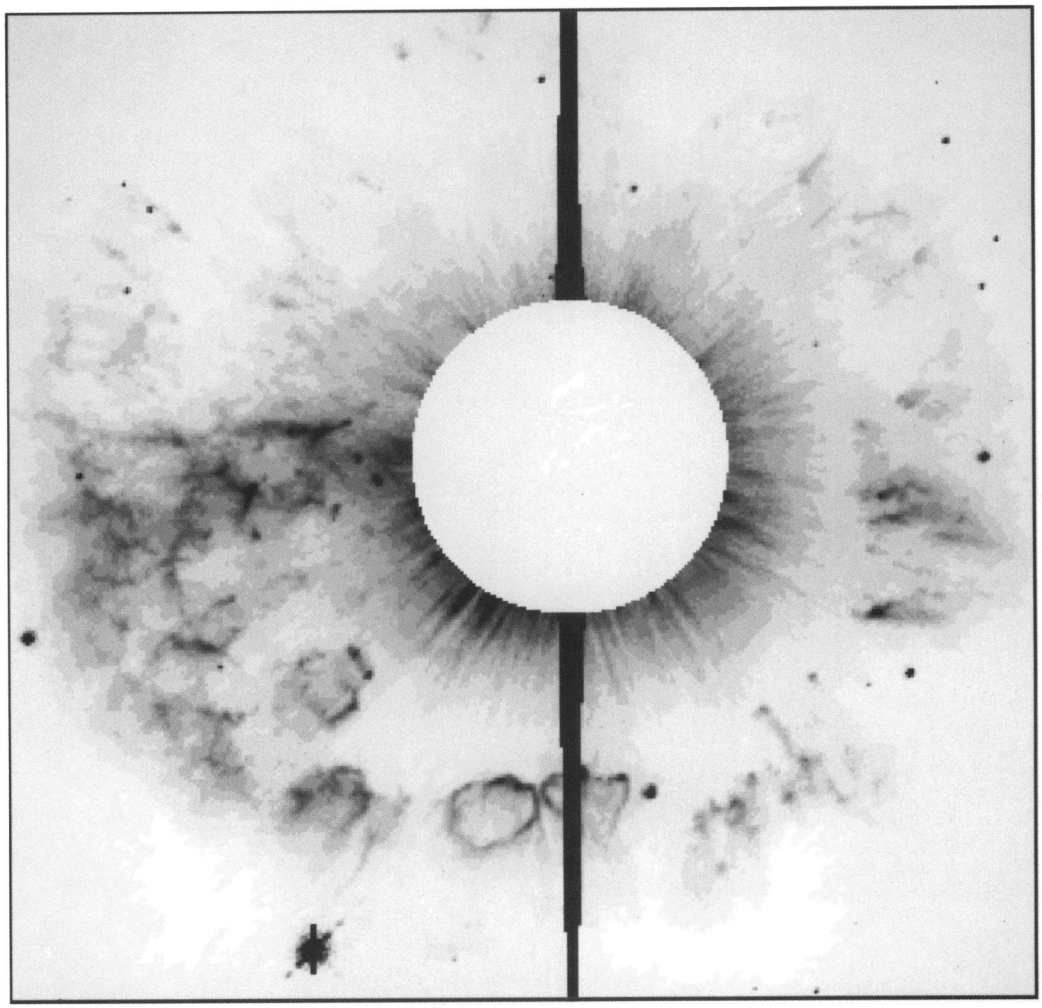

FIG. 9.—A 2000 s *HST*/WFPC2 image of AG Car taken in the F547M filter. North is in the lower right-hand corner. The field of view is the entire PC chip, 36″ × 36″.

NOTA et al. (see 448, 791)

2: 4.2 $M_\odot$ for AG Car, 3.1 $M_\odot$ for R127, 1.7 $M_\odot$ for S119. In addition to the ionized gas, the AG Car nebula shows the presence of dust. Smith et al. (1994) derive a dust mass for the nebula of 1.3×10^{-2} $M_\odot$. Smith et al. (1994) determine the nebular mass of He 3-519 to be $\simeq 2$ $M_\odot$, from the total Hα flux provided by Stahl (1987) (corrected for their recently derived nebular reddening, under the assumption of a temperature $T_e \simeq 8000$ K). He 3-519 also shows the presence of dust. From the color-corrected *IRAS* fluxes at 12, 25, and 60 μm, Smith et al. (1994) derive a dust mass 6.6×10^{-3} $M_\odot$, assuming a homogenous distribution of silicate grains at the same temperature of 73 K. In spite of its filamentary nature, HR Car is also surrounded by 2.1 $M_\odot$ of ionized gas. Much smaller, compared to the other LBVs, is the mass of the nebula around P Cyg: Barlow et al. (1994) derive an ionized gas mass of 9.3×10^{-3}, under the assumption of an electron temperature of 5000 K and an electron density of 1000 cm^{-3}. *IRAS* observations of P Cyg have been reanalyzed by Barlow et al. (1994) to establish whether dust is present in the star's circumstellar environment, but the results are inconclusive. In spite of the uncertainties, the estimated masses of the nebulae are consistent with the high mass-loss rates that are observed in the LBVs and with the nebular ages.

2.4. *Ionization Characteristics, Density, Temperature*

Most LBVNs appear to be totally ionized by the central star. In AG Car, for example, the radius of the Strömgren sphere easily encompasses the dimensions of the optical nebula, which is, therefore, density-bounded. It is to be noted that the recombination timescale is sufficiently long ($\simeq$250 yr) in comparison with the typical timescale associated with the recurrence of LBV variations, and therefore the nebula will remain ionized even when the star enters a phase of lower temperature. In this case, regions of higher density could show higher O^+/O^{++} (or N^+/O^{++}); unfortunately most LBVNs are O-poor, and O^{++} is not detected. The R127 nebula is also density-bounded, with a radius for the Strömgren sphere calculated to be 1.3 pc (Clampin et al. 1993) compared to the radius of the nebula of 0.9–1.1 pc.

HR Car is a borderline case: assuming the spectral type observed for the star (B2 I) (Hutsemekers & van Drom 1991a), the total output of ionizing photons in the Lyman continuum would be insufficient to ionize the entire nebula, but only the innermost 0.3 pc. HR Car would be, therefore, the only case of an LBVN which is radiation-bounded. On the other hand, in common with AG Car, the recombination timescale is of the order of 200 yr, very long compared to the typical timescale of LBV spectral variations (a decade). This means that if, during one of the previous minimum phases, HR Car had assumed a spectral type earlier than B2 I, as is observed for many other LBVs, the nebula would then have been completely ionized, and would remain ionized although the star itself had cooled down in the meantime.

Density and temperature characteristics are quite homogeneous across the sample. Usually, density information is derived from the [S II] λ6717/[S II] λ6731 intensity ratio, assuming a temperature which is derived from the [N II] 5755 Å line. Uncertainties affect these values: the density is usually measured averaging large regions; the 5755 Å line is faint and difficult to measure. Within the errors, the density appears to be relatively uniform across the LBVNs, ranging from about 300 cm^{-3} for He 3-519 to 100 cm^{-3} for R127. The temperatures are also uniformly on the low side, from 5000 K to a maximum of 12,500 K for HR Car.

3. THE UNIFIED PICTURE

The similarities in the properties and morphologies of the nebulae around LBVs (discussed in §§ 1 and 2) suggest the possibility of a unified picture for these objects.

In particular, the fact that most nebulae are axisymmetric (bipolar or elliptical) suggests that the shaping mechanism may involve a wind interacting with a "density contrast." In the context of this model, originally proposed for the shaping of planetary nebulae (Balick 1987; Soker & Livio 1989; Frank et al. 1993), a fast, spherically symmetric wind from the central star interacts, and "*snowplows*" into a preexisting "density contrast" between the equatorial and polar directions (material being denser at the equator). As a consequence, the fast wind can penetrate more easily in the polar direction, generating two bipolar "bubbles," while a narrower "waist" is compressed in the equatorial direction. *Depending on whether the density contrast is large or small, a pronounced bipolar or elliptical morphology (respectively) is generated.*

3.1. *A Qualitative Numerical Demonstration*

We shall discuss in § 3.2 below possible mechanisms for the generation of the density contrast, but first, in order to demonstrate the effects of the interaction of the fast wind with such a contrast qualitatively, we performed a highly simplified, two-dimensional numerical calculation, using a particle-in-cell description of the hydrodynamics. The method of calculation is similar to that used by Livio et al. (1986) and Soker & Livio (1989). We assumed an ad hoc density contrast profile of the form

$$\rho = \rho_0(1 + 5\cos^4\theta)\,, \qquad (1)$$

where θ is the angle to the equatorial plane, in a slowly moving ($V_{\rm slow} = 50$ km s^{-1}) wind, with a mass-loss rate of $\dot{M}_{\rm slow}$. About 250 yr after the end of the slow wind, we started a spherically symmetric fast wind, with $V_{\rm fast} = 10V_{\rm slow}$ $\dot{M}_{\rm fast} = 0.1\dot{M}_{\rm slow}$. The resulting morphology, 250 yr after the start of the fast wind, is shown in Figure 10. As can be seen, the results of the numerical calculations are strikingly similar to the morphology observed, for example, in the case of R127 (Fig. 3) (or AG Car, with an inclination of $\simeq$45°). If the R127 nebula can be used as a tracer of an earlier slow wind, then $V_{\rm slow}$ is indeed roughly given by the expansion velocity of the nebula ($\simeq$30 km s^{-1}). The star's current wind, on the other hand, gives us $V_{\rm fast}$, which for R127 is 260 km s^{-1}. It is interesting to notice that, given a choice of parameters similar to R127's, our numerical simulation produces a morphology clearly resembling the R127 nebula.

Recently, Frank, Balick, & Davidson (1995) performed a similar hydrodynamic calculation, with parameters appropriate for the η Car system (in particular including the eruption in the years 1840–1860). In order to generate the density contrast, they assumed the existence of a preeruption slow wind with a density ratio (equator to pole) of 100. During the eruption, Frank et al. (1995) assumed a mass-loss rate of $\dot{M}_E \sim 2 \times 10^{-2}$ $M_\odot$ yr^{-1} with a velocity of 800 km s^{-1}. This was followed by a posteruption phase of reduced mass loss ($\sim$10% if $\dot{M}_E$) at the same speed. Again, the results reproduce quite well the morphology observed in η Car. A density contrast of only 10 was found to be insufficient for reproducing well the narrowness of the observed "waist" (Fig. 4).

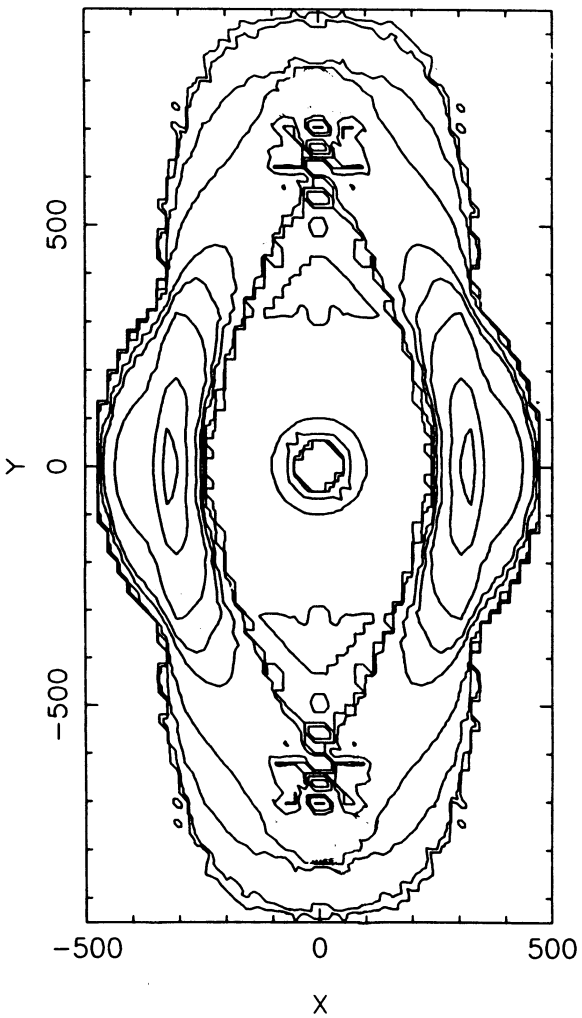

FIG. 10.—Density contours at time 250 yr after the start of the fast wind. The units on the axes are 10^{15} cm. The contours are in units of 10^{-22} g cm^{-3} between 3×10^{-4} and 20.

On the basis of the qualitative calculations presented here and the more refined calculations of Frank et al. (1995), as well as on the experience gained from calculations of the shaping of planetary nebulae (e.g., Frank et al. 1993), we suggest that the shaping of all the bipolar and elliptical nebulae around LBVs (e.g., η Car, AG Car, HR Car, R127, WRA 751) *is the consequence of the interaction of the fast wind with a density contrast.* The main distinguishing physical parameter determining the resulting morphology is the degree of the contrast (e.g., as measured by the equator-to-pole density ratio), *with a low contrast resulting in elliptical nebulae, while a high contrast produces strongly bipolar flows.*

3.2. *Possible Mechanisms for the Generation of the Density Contrast*

One of the main questions that arise in relation to our proposed model is what generates the background density contrast, into which the fast wind runs. There exist several possible mechanisms (in principle at least) for the generation of a density contrast (see also Livio 1995). We will briefly describe some of these mechanisms and discuss which of them may be more applicable.

3.2.1. *The Protostellar Disk*

One of the possibilities is that the density contrast is generated by the inner rim of a relic protostellar disk. Such a model has been suggested also for the generation of the morphology of the Egg Nebula (Pringle 1989), some bipolar planetary nebulae (e.g., Balick & Preston 1988), and the ring around SN 1987A (McCray & Lin 1994). There exist also other observational indications that circumstellar disks may exist around massive stars (e.g., observations of the B[e]-type star R126, by Zickgraf et al. 1985, and of MWC 349, by Welch 1993).

It can be expected that such a protostellar disk will generate a *very high* density contrast and a rather *narrow* (in terms of vertical extent) waist (these are in fact the two characteristics that led McCray & Lin 1994 to suggest this as a model for the ring in SN 1987A).

These conditions may be adequate for η Car but not for the other LBVs, where a moderate density contrast is indicated. It should also be noted, however, that η Car is younger than the other systems. Since the morphology can be expected to evolve, it may be that very young nebulae exhibit a more pronounced bipolar structure.

Some of the material that appears to be ejected in the "*waist*" area at high velocities could represent fragments of this preexisting disk (see § 2.1); however, this interpretation is not unique (see § 3.2.2 below).

3.2.2. *An Equatorially Compressed Outflow*

In a recent work, Bjorkman & Cassinelli (1992, 1993) proposed that winds from rapidly rotating early-type stars are strongly focused toward the equatorial plane, forming an equatorially compressed outflow. This suggestion has been confirmed by detailed hydrodynamic simulations (Owocki, Cranmer, & Blondin 1994). The important parameter, determining whether or not an equatorially compressed outflow forms, was found to be the ratio of the equatorial rotation velocity, $V_{\rm rot}$, to the wind velocity at a large distance, V_∞ (see also Livio 1994). The threshold value was found to be $V_{\rm rot}/V_\infty \gtrsim 0.25$ (depending somewhat on $V_\infty/V_{\rm esc}$, where $V_{\rm esc}$ is the escape velocity from the stellar surface). The following important results emerge from these calculations.

1. The equatorial outflow was found to produce density contrasts (for $V_{\rm rot}/V_\infty$ above the threshold) as high as $\rho_{\rm disk}/\rho_{\rm pole} \sim 300$ (depending on the input physical parameters).
2. The radial outflow velocity at the equator was found to be smaller than that near the pole by a factor of a few (at the maximum distance of the calculation, of about 6 polar radii). The second point is extremely important, because, for a waist to be formed (e.g., as in the simulation by Frank et al. 1995 of the η Car system; see § 3.1), the fast, spherically symmetric wind must be able to "catch up" with the slower wind which forms the density contrast.

This mechanism can therefore generate both high and low density contrasts, depending on the system parameters. As already mentioned, for some choice of the parameters, the configuration observed in η Car can be reproduced. The high-velocity material that is observed in the equatorial plane could represent cold matter in the equatorially compressed outflow, that has been accelerated by the wind ejected in the outburst. For this mechanism to work, however, the star must be relatively rapidly rotating.

3.2.3. *An Asymmetric Red Supergiant Wind*

Several authors have suggested that (at least some) LBVs have passed through a yellow/red supergiant phase (e.g., Robberto et al. 1993). If that is really the case, then it is possible that the shaping mechanism is similar to the one that probably operates in planetary nebulae. The idea is that during the red supergiant phase, a slow wind is emitted. In the subsequent blue supergiant phase, the fast wind ($V_W^{\rm blue}$ roughly a few hundred km s^{-1}) catches up with the slow wind, shocks it, and "snowplows" into it. If, for whatever reason (see below), the slow wind is denser near the equator than at the poles, then an elliptical or bipolar morphology will be found (depending on the density contrast; Balick 1987, Frank et al. 1993).

The question that still needs to be addressed is, *What are the mechanisms that can generate a density contrast in the red supergiant wind*?

Probably the most promising mechanism is related to the presence of a binary companion (e.g., Livio 1993, 1994 and references therein).

A binary companion can spin up the red supergiant envelope either via a common envelope phase (see Iben & Livio 1993 for a review) or via tidal interactions, to the point that the critical rotation for the generation of an equatorially compressed outflow (§ 3.2.2 above) will be obtained. Similarly, in a common envelope phase, mass from the envelope is ejected preferentially in the orbital plane (e.g., Terman, Taam, & Hernquist 1994; Livio & Soker 1988), again generating a density contrast.

The degree of contrast that can be obtained by such a mechanism (if a red supergiant phase indeed occurs) depends on the binary system parameters (e.g., a more massive secondary can be expected to form a higher contrast). For this mechanism to operate, it is necessary for the LBVs to have experienced a slow-wind evolutionary phase.

3.3. *The Possible Role of Magnetic Fields*

Magnetic fields are always a possible agent for the formation of axisymmetric configurations. In particular, the fact that the toroidal component of the magnetic field in the wind from a rotating star becomes increasingly important with the distance from the star (e.g., Brandt 1970) suggests the possibility of an axisymmetric flow. In a recent work, Chevalier & Luo (1994) have shown that in the bubble generated when a fast wind shocks against an external medium, the toroidal field can dominate over the thermal pressure. A bipolar flow was obtained, due to the fact that magnetic tension can constrain the flow in the equatorial direction (while it has no effect in the polar direction). Chevalier & Luo (1994) found that significant magnetic effects on the nebula require a surface magnetic field of at least

$$B_S^{\rm min} = 25\left(\frac{\sigma}{10^{-4}}\right)^{1/2}\left(\frac{\dot{M}}{10^{-3}\ M_\odot\ {\rm yr}^{-1}}\right)^{1/2}\left(\frac{V_{\rm FW}}{500\ {\rm km\ s}^{-1}}\right)^{1/2} \times \left(\frac{R_S}{7\times 10^{12}\ {\rm cm}}\right)^{-1}\left(\frac{V_{\rm rot}/V_{\rm FW}}{0.1}\right)^{-1}{\rm G}\,, \quad (2)$$

where σ is the ratio of the field energy density to the kinetic energy density in the wind, R_S is the stellar radius, $V_{\rm FW}$ is the velocity of the fast wind, and $V_{\rm rot}$ is the equatorial surface rotational velocity of the star.

The basic picture is again that of a fast wind running into a slower wind (which was generated in a previous phase), generating a shell which moves at approximately constant velocity. It was found that the obtained morphology (which was always axisymmetric) depends on two parameters: $\eta \equiv \sigma V_{\rm FW}/V_S$, where V_S is the shell velocity in the polar direction, and $\lambda \equiv V_{\rm SW}/V_S$, where $V_{\rm SW}$ is the velocity of the slow wind. For small values of λ an equatorial ring is formed, while for larger values of λ a double-lobe structure is obtained. The operation of this mechanism depends on the presence of a strong enough magnetic field (which satisfies condition [2]). It is important to note, from equation (2), that if the star is a slow rotator, the requirement on the magnetic field strength may become difficult to satisfy. Binary companions may again help in this respect, since the companion can (by tidal interaction or common envelope evolution) spin up the envelope. Unfortunately, no observational data exist on magnetic fields in LBVs.

3.4. *The Interacting Winds Scenario and the Small-Scale Structures*

In addition to explaining the observed morphologies on a large scale, an interacting winds scenario can help to understand some of the small-scale structures observed in LBVNs. As already mentioned in the previous sections, η Car's bipolar lobes appear very clumpy in the recent *HST* pictures. P Cyg's nebula is almost exclusively composed by clumps, and clumps were present in the ground-based pictures of AG Car. In the new *HST* pictures of AG Car, where the clumps are resolved for the first time, they seem shaped by the action of a fast wind, assuming in many cases the appearance of cometary tails. LBV shells are highly unstable to a ram-ram pressure mechanism (García-Segura, Mac Low, & Langer 1994). Such an instability is referred to as a *nonlinear thin-shell instability* in Vishniac (1994), and it operates in dense winds, where the cooling is efficient enough to make radiative terminal shocks. A similar instability has also been found recently in colliding winds for binary systems (Stevens, Blondin, & Pollock 1992), when both terminal shocks are isothermal. When the LBV wind ($V_{\rm fast}$) collides with the previous wind ($V_{\rm slow}$), it produces a postshock gas at high temperature ($\simeq 10^6$ K), but the high density of this wind enables the gas to cool rapidly, producing a radiative isothermal shock. As soon as the LBV wind produces a swept-up shell, it forms ripples from the local irregularities of the previous wind. The ripples introduce an inhomogeneous radial velocity field in the shell, and free-streaming gas can pass throughout the faster parts of the shell. The slower parts are generally clumps forming regions: when the slower clumps are exposed to the incoming wind, bow shocks are formed around them (G. García-Segura 1994, private communication; see also Dyson, Hartquist, & Biro 1993), generating the observed cometary tails.

4. CONCLUSIONS

We have examined in detail the properties of the nebulae around a number of LBVs and candidates, by compiling the results of our ground-based coronagraphic imaging and spectroscopic study, together with information available in the literature. First, we have considered their morphologies. All of the LBVNs discussed except one (P Cyg) exhibit a clearly axisymmetric structure. In addition, they generally appear as either a shell or a filamentary nebula. In order to address similarities and differences comprehensively, we have therefore defined two distinct morphological classes. For the sake of

completeness, we have defined a third category, peculiar nebulae, which contains only one object, P Cyg, for which none of the above statements are valid, since its nebula is neither axisymmetric, shell-like nor filamentary, and it is not discussed in detail in this paper.

In addition to the morphology, we have reviewed and compared a number of characteristic parameters such as the mass, temperature, density, ionization, expansion velocity, and dynamical timescale. Overall, the comparison indicates a relatively homogeneous sample of low-ionization nebulae, mostly density-bounded with a few solar masses of ionized hydrogen, similar densities, velocities of the order of tens of kilometers per second, and similar dynamical timescales of $\simeq 10^4$ yr. The homogeneity of their properties provides a strong argument in favor of a single formation mechanism. In addition, the fact that the large majority exhibit clear axisymmetries suggests that the nebular shaping mechanism, in analogy to planetary nebulae (Balick 1987), might involve an interacting winds scenario.

We, propose, therefore, that a model which consists of a stellar wind interacting with a preexisting density contrast (between the equatorial and polar directions) can explain most of the observed morphologies: a large density contrast would generate a pronounced bipolar structure, while a smaller density contrast would result in a more elliptical morphology. This hypothesis is supported by a qualitative numerical simulation which uses input parameters consistent with the wind and nebular characteristics observed in our sample of LBVs.

There are several mechanisms which can produce the necessary density contrast, ranging from the presence of a protostellar disk, a relic of the pre–main-sequence evolution, to an asymmetric red supergiant wind from an earlier phase. We have reviewed these scenarios qualitatively and conclude that it is difficult to determine definitively at this time whether one or more of these mechanisms have been operating in the different systems. In contrast to PNe, the statistical significance of our sample of LBVs and candidates is limited, and the information available is not complete, although significant progress has been recently made. More observations are needed to confirm the LBV nature of the candidates and establish new members of the class. In parallel, a more quantitative analysis of the models presented here is required. We are planning to address the latter in work which is currently in progress.

The authors wish to thank the referee, Bruce Balick, for interesting comments. A. N. thanks Guillermo García-Segura for the many discussions and some unpublished material. M. C. acknowledges the STScI DDRF for continuing funding of the Coronagraph Project. M. L. acknowledges support from NASA grant NAGW-2678.

REFERENCES

Allen, D. A., & Hillier, D. J. 1993, Proc. Astron. Soc. Australia, 10, 338
Appenzeller, I., Wolf, B., & Stahl, O. 1987, in Instabilities in Luminous Early-Type Stars, ed. C. de Loore & A. Willis (Dordrecht: Reidel), 241
Balick, B. 1987, AJ, 94, 671
Balick, B., & Preston, H. L. 1988, AJ, 94, 958
Barlow, M., Drew, J. E., Meaburn, J., & Massey, R. M. 1994, MNRAS, 268, L29
Bjorkman, J. E., & Cassinelli, J. P. 1992, in Nonisotropic and Variable Outflows from Stars, ed. L. Drissen, C. Leitherer, & A. Nota (San Francisco: ASP), 88
———. 1993, ApJ, 409, 429
Bohannan, B., & Walborn, N. 1989, PASP, 101, 520
Brandt, J. C. 1970, Introduction to the Solar Wind (San Francisco: Freeman)
Caputo, F., & Viotti, R. 1970, A&A, 7, 266
Chevalier, R. A., & Luo, D. 1994, ApJ, 421, 225
Chu, Y.-H. 1993, in IAU Symp. 155, Planetary Nebulae, ed. R. Weinberger & A. Acker (Dordrecht: Kluwer), 139
Clampin, M., Nota, A., Golimowski, D., Leitherer, C. & Durrance, S. 1993, ApJ, 410, L35
Clampin, M., Nota, A., Robberto, M., Paresce, F., & Staude, J. 1995a, in preparation
Clampin, M., Schulte-Ladbeck, R., Nota, A., Robberto, M., Paresce, F., & Clayton, G. C. 1995b, AJ, in press
Conti, P. S. 1984, in Observational Tests of Stellar Evolution Theory, ed. A. Maeder & A. Renzini (Dordrecht: Reidel), 233
Davidson, K. 1987, in Instabilities in Luminous Early-Type Stars, ed. H. J. G. L. M. Lamers & C. W. H. de Loore (Dordrecht: Reidel), 127
———. 1989, in IAU Colloq. 113, Physics of Luminous Blue Variables, ed. K. Davidson, A. F. J. Moffat, & H. J. G. L. M. Lamers (Dordrecht: Kluwer), 101
Davidson, K., Dufour, R. J., Walborn, N. R., & Gull, T. R. 1986, ApJ, 254, L47
Davidson, K., Humphreys, R. M., Hajian, A., & Terzian, Y. 1993, ApJ, 411, 336
De Groot, M. 1969, Bull. Astron. Inst. Netherlands, 20, 235
de Koter, A. 1993, Ph.D. thesis, Univ. Utrecht
de Winter, D., Perez, M. R., Hu, Y. H., & The, P. S. 1992, A&A, 257, 632
Dyson, J. E., Hartquist, T. W., & Biro, S. 1993, MNRAS, 261, 430
Ebbets, D., Garner, H., White, R., Davidson, K., Malumuth, E., & Walborn, N. 1993, in Circumstellar Media in the Late Stages of Stellar Evolution, ed. R. Clegg et al. (Cambridge: Cambridge Univ. Press), 95
Ebbets, D., White, R., Walborn, N., Davidson, K., & Malumuth, E. 1992, in ESO Conf. Proc., Science with the *Hubble Space Telescope*, ed. P. Benvenuti & E. Schreier (Garching: ESO), 395
Exter, K. 1994, Master's thesis, Univ. Manchester
Frank, A., Balick, B., & Davidson, K. 1995, ApJ, 441, L77
Frank, A., Balick, B., Icke, V., & Mellema, G. 1993, ApJ, 404, L25
García-Segura, G., Mac Low, M., & Langer, N. 1994, A&A, in preparation
Hu, J. H., de Winter, D., The, P. S., & Perez, M. R. 1990, A&A, 227, L17
Humphreys, R. M. 1989, IAU Colloq. 113, Physics of Luminous Blue Variables, ed. K. Davidson, A. F. J. Moffat, & H. J. G. L. M. Lamers (Dordrecht: Kluwer), 3
Humphreys, R. M., & Davidson, K. 1994, PASP, 106, 1025
Humphreys, R. M., Lamers, H., Hoekzema, N., & Cassatella, A. 1989, A&A, 218, L17
Hutsemekers, D. 1994, A&A, 281, L81
Hutsemekers, D., & Van Drom, E. 1991a, A&A, 248, 141
Hutsemekers, D., Van Drom, E., Gosset, E., & Melnick, J. 1994, A&A, in press
Iben, I., Jr., & Livio, M. 1993, PASP, 105, 1373
Lamers, H. J. G. L. M. 1987, in Instabilities in Luminous Early-Type Stars, ed. H. J. G. L. M. Lamers & C. W. H. de Loore (Dordrecht: Reidel), 99
Lamers, H. J. G. L. M., Korevaar, P., & Cassatella, A. 1985, A&A, 149, 29
Langer, N., Hamann, W.-R., Lennon, M., Najarro, F., Pauldrach, A. W. A., & Puls, J. 1994, A&A, 290, 819
Leitherer, C., et al. 1994, ApJ, 428, 292
Leitherer, C., Schmutz, W., Abbott, D. C., Hamann, W. -R., & Wesselowski, U. 1989, ApJ, 346, 919
Livio, M. 1993, in IAU Symp. 155, Planetary Nebulae, ed. R. Weinberger & A. Acker (Dordrecht: Kluwer), 279
———. 1994, in Circumstellar Media in the Late Stages of Stellar Evolution, ed. R. Clegg et al. (Cambridge: Cambridge Univ. Press), 35
——. 1995, in Asymmetrical Planetary Nebulae, ed. A. Harpaz & N. Soker (Bristol: IOP), 51
Livio, M., & Soker, N. 1988, ApJ, 329, 764
Livio, M., Soker, N., de Kool, M., & Savonije, G. J. 1986, MNRAS, 222, 235
McCray, R., & Lin, D. N. C. 1994, Nature, 369, 378
Mila Mitra, P., & Dufour, R. J. 1990, MNRAS, 242, 98
Nota, A., Clampin, M., Leitherer, C., & García-Segura, G. 1995, in preparation
Nota, A., Drissen, L., Clampin, M., Leitherer, C., Pasquali, A., Robert, C., Paresce, F., & Robberto, M. 1994, in Circumstellar Media in the Late Stages of Stellar Evolution, ed. R. Clegg et al. (Cambridge: Cambridge Univ. Press), 89
Nota, A., Leitherer, C., Clampin, M., Greenfield, P., & Golimowski, D. A. G. 1992, ApJ, 398, 621
Owocki, S. P., Cranmer, S. R., & Blondin, J. M. 1994, ApJ, 424, 887
Panagia, N., Gilmozzi, R., Macchetto, F., Adorf, H.-M, & Kirshner, R. P. 1992, ApJ, 380, L23
Parker, J. W., Clayton, G. C., Winge, C., & Conti, P. S. 1993, ApJ, 409, 770
Pringle, J. E. 1989, MNRAS, 238, 37P
Robberto, M., Ferrari, A., Nota, A., & Paresce, F. 1993, A&A, 269, 3330
Schwarz, H. E., Corradi, R. L. M., & Melnick, J. 1992, A&AS, 96, 23
Smith, L. 1991, in IAU Symp. 143, Wolf-Rayet Stars and Interrelations with Other Massive Stars in Galaxies, ed. K. A. van der Hucht & B. Hidayat (Dordrecht: Kluwer), 385
Smith, L. J., Crowther, P. A., & Prinja, R. K. 1994, A&A, 281, 833
Soker, N., & Livio, M. 1989, ApJ, 339, 268
Stahl, O. 1986, A&A, 164, 321
———. 1987, A&A, 182, 229

Stahl, O., & Wolf, B. 1986, A&A, 158, 371
Stevens, I. R., Blondin, J. M., & Pollock, A. M. T. 1992, ApJ, 386, 285
Taylor, M., Nordsieck, K. H., Schulte-Ladbeck, R. E., & Bjorkman, K. S. 1991, AJ, 102, 1197
Terman, J. L., Taam, R. E., & Hernquist, L. 1994, ApJ, 422, 729
Thackeray, A. D. 1950, MNRAS, 110, 526
van Genderen, A. M. 1989, A&A, 208, 135
Vishniac, E. T. 1994, ApJ, 428, 186
Walborn, N. R. 1977, ApJ, 215, 53
Walborn, N. R., & Blanco, B. M. 1988, PASP, 100, 797
Walborn, N. R, Blanco, B. M., & Thackeray, A. D. 1978, ApJ, 219, 498
Welch, Wm. J. 1993, in ASP Cont. Ser. 35, Massive Stars: Their Lives in the Interstellar Medium, ed. J. P. Cassinelli & B. Churchwell (San Francisco: ASP), 15
Wolf, B. 1989, A&A, 217, 87
Wolf, B., Stahl, O., Smolinski, J., & Cassatella, A. 1988, A&AS, 74, 230
Zickgraf, F. J., Wolf, B., Stahl, O., Leitherer, C., & Klare, G. 1985, A&A, 143, 241